JOURNAL OF MAGNETIC RESONANCE **125,** 140–144 (1997)
ARTICLE NO. MN961068

NOTES

High-Resolution Spectra of Liposomes Using MAS NMR. The Case of Intermediate-Size Vesicles

MOUNIR TRAIKIA, DENIS B. LANGLAIS,* GINA M. CANNAROZZI, AND PHILIPPE F. DEVAUX†

Laboratoire de Biophysique Cellulaire, Université Denis Diderot, Couloir 23-13, 5 ème, 2 Place Jussieu, 75251 Paris Cedex 5, France

Received August 6, 1996; revised November 4, 1996

The acquisition of high-resolution spectra of large unilamellar vesicles has been hampered by problems of line broadening caused by lipid and vesicle motion in the intermediate motional regime. In this paper, we introduce a method for obtaining ^{31}P NMR high-resolution spectra of large unilamellar vesicles by slowing the vesicle dynamics into a more tractable time scale.

Traditional models of biological membranes for NMR studies include multilamellar vesicles (MLVs) which can range in size from 0.2 to 10 μm (*1, 2*), small unilamellar vesicles (SUVs) with diameters of approximately 20–40 nm (*3*), and large unilamellar vesicles (LUVs) with diameters from 50 to 200 nm (*4, 5*). The many-layered MLVs have been widely exploited for structural and motional information (*6–9*). Because of their large size, there is little averaging of the anisotropic part of the spin Hamiltonian by vesicle tumbling, making them well adapted to study by wideline solid-state NMR techniques. Indeed, order parameters deduced from wideline ^{2}H or ^{31}P NMR spectra as well as lineshape simulations have provided a wealth of information on the dynamics and conformation of lipids in membranes.

For several types of investigations, such as membrane permeability, drug delivery by liposomal encapsulation (*10, 11*), and membrane fusion (*12*), however, unilamellar vesicles are preferable. SUVs, generally obtained by sonication of MLVs, have been used as model membranes when the need for unilamellarity is paramount. SUVs give rise to high-resolution spectra as their fast rotational motion averages the anisotropic dipolar interaction to zero and the chemical shift to its isotropic value (*13–20*). However, the high curvature of the SUVs always raises the question of biological relevance.

Intermediate-size LUVs, which can be obtained by a rapid extrusion procedure, offer an attractive combination of low curvature and unilamellarity. Their unilamellarity is particularly advantageous for biotechnological applications, while their small curvature makes them better models for biological membranes than the highly curved SUVs. However, as the vesicle size increases from that of the SUVs, the membrane tumbling becomes progressively slower (*21*) and the efficiency of the orientation averaging by lateral diffusion decreases because of the low curvature of the vesicles. The time scale of the molecular tumbling of the LUVs falls into the intermediate time scale regime. The tumbling of the vesicles is too slow to average out the anisotropic interactions: the spectra have powder lineshapes distorted by partial averaging (*21, 22*). Thus, the LUV spectra are not motionally averaged to high resolution like SUVs, and in addition, they cannot be spun to high resolution with MAS like the MLVs (*23–26*). The molecular tumbling in the intermediate regime diminishes the efficiency of the lineshape averaging (*27, 28*). Here, we show a method to evade this ''incoherent averaging'' effect by reducing the vesicles overall motion and thus moving the vesicles' dynamics out of the intermediate motional regime.

Egg phosphatidylcholine (EPC), egg phosphatidylglycerol (EPG), egg phosphtidylethanolamine (EPE), cholesterol (CHOL), and 1,2-dioleoyl-sn-glycero-3-phosphocholine (DOPC) were purchased from Sigma Chemical Co. and were used without further purification. 1,2-Dioleoyl-sn-glycero-3-phosphate (DOPA) was synthesized in our laboratory from DOPC following the procedure of Roux *et al.* (*29*). The purity of these lipids was checked by thin-layer chromatography and by high-resolution NMR in chloroform. The buffer used in the experiments was 100 m*M* *N*-[2-hydroxyethyl]piperazine-*N*′-[ethanesulfonic acid] (Hepes), 100 m*M* potassium sulfate (K_2SO_4) and 5 m*M* ethylendiamine tetraacetic acid (EDTA).

To prepare the liposomes, the appropriate proportions of lipids were dissolved in 3 ml of chloroform and 1 ml of methanol to ensure homogenous mixing. The solvent was slowly removed at room temperature by rotary evaporation.

† To whom correspondence should be addressed.
* Present address: Physics Department, Simon Fraser University, Burnaby, BC V3J 1J2 Canada

1090-7807/97 $25.00

The film was dried in high vacuum for at least 2 h and then hydrated with 1 ml of the buffer solution. The MLVs were obtained by five cycles of freeze/thawing with liquid nitrogen and a 50°C water bath followed by vortexing. To ensure that the samples were identical, the LUV samples were obtained by multiple passages of the MLV through an extruder produced by Sciema Technical Services Ltd. (Richmond, BC) equipped with polycarbonate filters (Nucleopore Corp., Pleasanton, CA). One-hundred nanometer vesicles were extruded twice with 1 μm, 400 nm, and 200 nm filters and 10 times with 100 nm filters (*5*).

The SUVs were prepared by sonication of the same MLV dispersion under a stream of argon using a probe-type sonicator (model VC50, Bioblock Scientific) at 40 W in an ice-bath with sonication periods of 2 min followed by rest periods of 2 min until a clear solution was obtained. The glycerol was added to the LUV and the mixture vortexed to make a uniform solution which was then placed in a NMR rotor.

All experiments were performed and processed on a Bruker AMX400-WB NMR spectrometer (^{1}H resonance at 400 MHz, ^{31}P resonance at 162 MHz) using a Bruker MAS probe with an external lock. The samples were contained in 4 mm ZrO_2 rotors ($\approx$110 μl of sample), the spinning speed was controlled to within 5 Hz at values varying between 2 and 14 kHz, and the temperature was verified at each speed using the chemical shifts of methanol protons (*30*) and by checking the temperature of the gel to liquid-crystalline phase transition for DMPC (23°C) and DPPC (41°C). The ^{31}P (90°) pulse length was 4.6 μs and the recycle delay was 2 s. The typical ^{31}P spectral width was 20 ppm (3.24 kHz). ^{1}H decoupling was not applied during acquisition of the ^{31}P magnetization. In all the experiments, 4096 complex points were acquired. Prior to Fourier transformation, the data were zero filled to 8192 points, exponentially multiplied with 10 Hz line broadening, and treated with automatic baseline correction.

The static spectrum of MLVs made from a concentrated suspension of EPC (200 mg/ml) is an axially symmetric powder pattern with a linewidth of 50 ppm (8 kHz) (not shown). Spinning the MLVs at the magic angle at 2 kHz was sufficient to reduce the linewidth to approximately 0.2 ppm as shown in Fig. 1 (closed triangles). The spectrum of 100 nm LUVs shows a broad asymmetrical ^{31}P peak with an approximate peak width of 15 ppm (2.5 kHz) (not shown). The LUV sample was spun at the magic angle at 30°C, and spectra were acquired at 10 different spinning speeds from 2 to 10 kHz. As the spinning speed increased, the linewidth decreased asymptotically to about 2 ppm as indicated in Fig. 1 (open circles). Decoupling had no effect under these conditions while an increase in temperature increased the linewidth by a few percent. Thus, the spontaneous tumbling of the LUVs interferes with the averaging caused by spinning the sample at the magic angle. In order to improve the efficiency of the averaging in this case, it was necessary to reduce the rotational motion of the vesicles by partial immobilization of the LUVs.

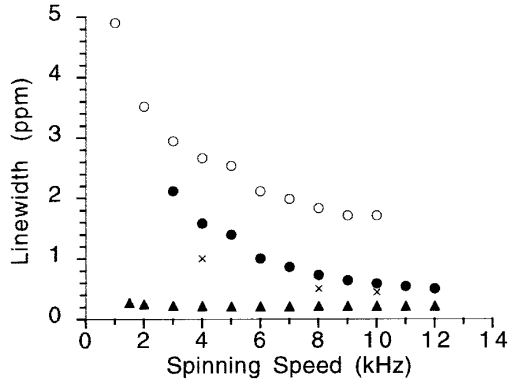

FIG. 1. ^{31}P linewidth of EPC vesicles as a function of spinning speed ν_r: (○) 100 nm LUVs at 30°C without glycerol; (●) 100 nm LUVs at 8°C with 50% glycerol; (×) 100 nm LUVs containing a mixture of EPC and cholesterol (4/1 mol ratio) at 8°C with 50% glycerol; and (▲) MLVs at 8°C and without glycerol.

Spectra of EPC LUVs in 50% glycerol at 8°C were acquired at 10 different spinning speeds and the corresponding linewidths are shown as closed circles in Fig. 1. As shown in this figure, at high spinning speeds (8–10 kHz), the linewidth of EPC in LUVs decreased significantly: for a spinning speed of 10 kHz, the linewidth decreased from 1.7 ppm at 30°C in the absence of glycerol to 0.6 ppm at 10 kHz with 50% glycerol at 8°C. As the viscosity is increased by decreasing the temperature or increasing the glycerol content, the linewidth decreases.

The MAS spectra of 100 nm LUVs composed of EPC/cholesterol (4:1, mol ratio) in 50% glycerol at 8°C show smaller linewidths than those in the absence of cholesterol (Fig. 1). Cholesterol is known to increase the viscosity of a lipid bilayer in the liquid crystalline phase, and to decrease the lateral diffusion of the lipids (*7, 9*). In conclusion, reducing the dynamics of the lipids in the LUVs (tumbling and diffusion) favors averaging by MAS.

The spectra of Fig. 2, obtained with an equimolar mixture of three phospholipids, EPG/EPE/EPC, illustrate the differences of resolution between the various conditions. Figure 2a shows the spectrum of MLVs at 8°C and 12 kHz spinning speed. The peaks are well resolved, with a linewidth of 0.2 ppm. The assignments to EPG, EPE, and EPC, respectively, were made by comparison with the spectra in organic solvent. Figure 2b shows the spectrum of the same lipid mixture in 100 nm LUVs, at the same spinning speed. The temperature was raised to 40°C in an unsuccessful hope to improve the resolution. Figure 2c shows the dramatic improvement in resolution obtained with this type of LUVs after adding 50% glycerol and decreasing the temperature to 8°C. The linewidth of the LUV resonances is now 0.4 ppm. Finally, the lipid peaks in the SUV spectrum at 30°C have linewidths of 0.3 ppm (Fig. 2d).

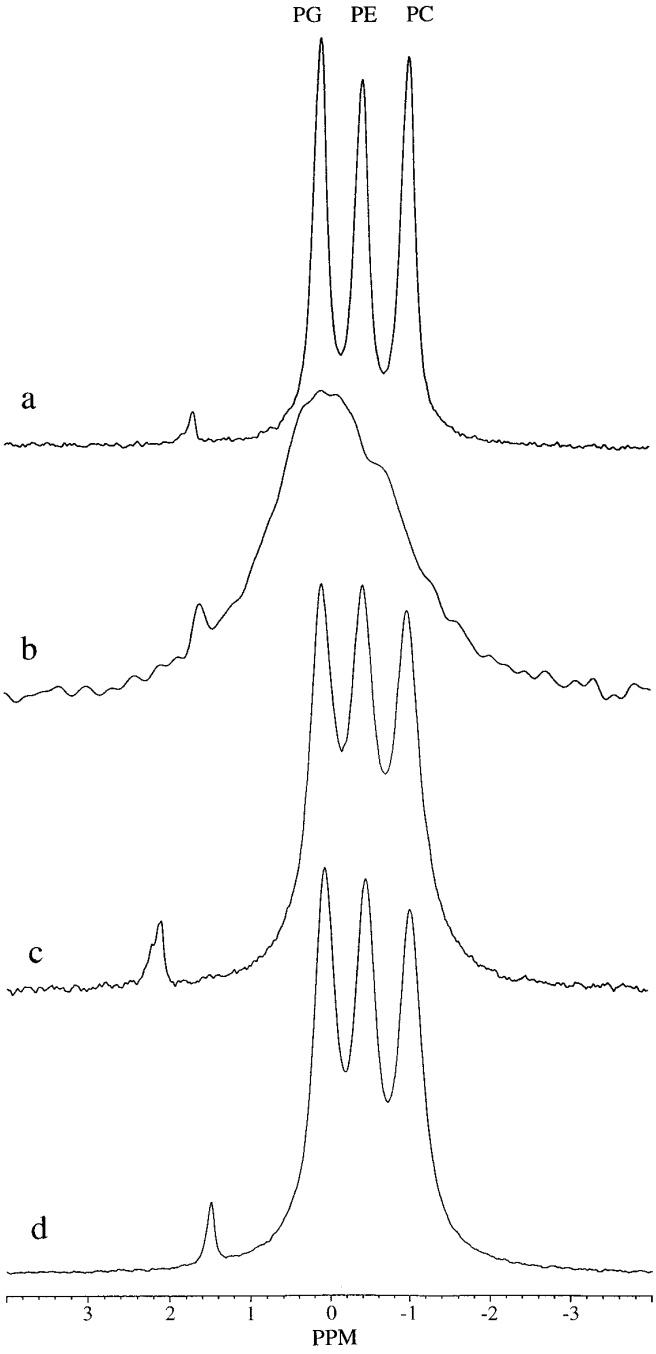

FIG. 2. 162 MHz ^{31}P NMR spectra of approximate equimolar mixture of EPG/EPE/EPC, 50 mg of total lipid per milliliter: (a) MLVs at 8°C, ν_r = 12 kHz, 2K scans; (b) 100 nm LUVs at 40°C, ν_r = 12 kHz, 3K scans; (c) 100 nm LUVs in 50% Glycerol at 8°C, ν_r = 12 kHz, 20K scans; (d) SUVs at 30°C, no spinning, 20K scans. Spectra (a, b, d) were recorded at pH 7.0, spectrum (c) at pH 7.5. The low field peak around 1.5 ppm is inorganic phosphate used to calibrate the pH.

To further illustrate the resolution enhancement obtained by cooling LUVs at low temperature in the presence of glycerol, samples containing dioleoyl-phosphatidic acid (DOPA) and DOPC (1:4 mol ratio) were made. The chemical shift of the phosphate moiety of DOPA is a function of both the local pH and the curvature of the vesicles (*19*). Consequently, in sonicated vesicles with a radius of approximately 20 nm, the inner and outer monolayers exhibit different chemical shifts and two peaks are seen for the PA in SUVs (Fig. 3a). It was inferred by Swairjo *et al.* that MLVs would give a single peak for PA on the inner and outer

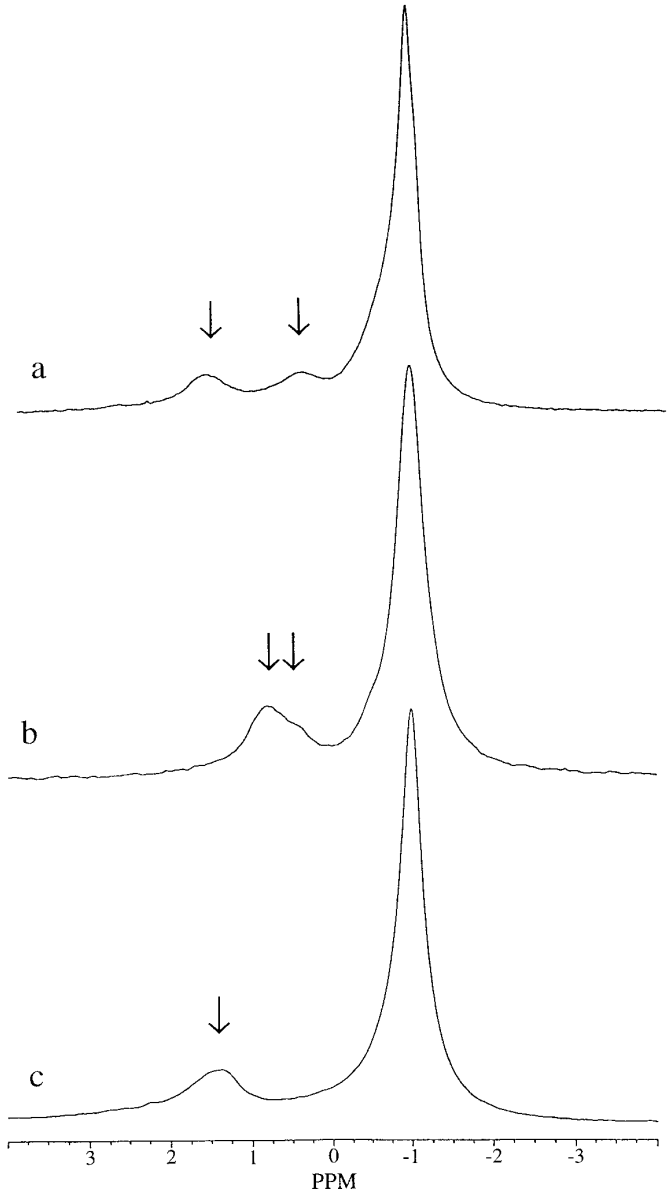

FIG. 3. Comparison of 162 MHz ^{31}P NMR spectra of vesicles comprised of DOPA:DOPC (−1:4), 18K scans: (a) SUVs without glycerol, 45°C, no spinning, pH 7.9; (b) 100 nm LUVs in 50% glycerol at 8°C, ν_r = 8 kHz, pH 7.5; (c) MLVs without glycerol, 8°C, ν_r = 8 kHz, pH 7.9. The vertical arrows emphasize the fact that on spectra (a) and (b) there are two peaks for PA corresponding to the inner and outer monolayers of SUVs or LUVs. There is only one PA peak in the case of MLVs.

monolayers because of their low curvature. Further, deconvolution of the broad PA peak from the spectrum of 50 nm LUVs (without spinning at the magic angle) brought these authors to conclude that the two leaflets of LUVs were also equivalent. However, Fig. 3b shows that with our technique PA, in 100 nm LUVs, gives rise to two peaks with a difference in chemical shift smaller than that of the SUVs. This shows, that even with the intermediate-sized vesicles, the two leaflets are still asymmetric but not to the same extent as the SUVs. Figure 3c shows only one peak for the PA and confirms the conclusion of Swairjo *et al.* that the curvature of both bilayer leaflets is equivalent in MLVs.

The problem of obtaining high-resolution spectra of dynamic systems using MAS was recognized by Maricq and Waugh in the mid-1970s when they described MAS using average Hamiltonian theory (*27*). They explained the effect of having two sources of dynamics, the mechanical spinning of the sample, and the rotation of the spin system, in our case the LUV. In a static powder sample without any internal dynamics, the averaging of the interaction is a result of the very specific path followed by the spins during the rotation and the refocusing of their magnetization after each rotation. If there are internal dynamics, the magnetization refocusing can be scrambled by specific spins moving from their original state during the rotation and thus no longer being refocused after one full rotation. Long *et al.* observed this type of interference effect between dynamics and RF pulse sequences in the spectra of a hopping $-NH_3$ (*28*). They observed changes in the lineshape that depended on the rate of motion caused by a change of temperature of the sample. Similarly, chemical exchange also causes lineshape changes in MAS experiments.

In the case of very large lipid vesicles (MLVs), spinning the sample at a few kilohertz is sufficient to obtain narrow peaks even though the spectrum of an immobilized phosphate is about 30 kHz wide. The fast axial reorientation of the phospholipid in the fluid ($L\alpha$) phase contributes to the averaging of the chemical shielding anisotropy by replacing the true time-dependent Hamiltonian describing the spin state of the phosphate by a time-averaged Hamiltonian with axial symmetry. The CSA in this effective Hamiltonian is not completely averaged to zero in the absence of sample spinning, because the fast motion of the head group is restricted to a certain angular domain. Spinning the MLVs at the magic angle, with a spinning speed of a few kilohertz, is then sufficient to obtain complete averaging.

In the case of smaller vesicles (LUVs and SUVs), with a diameter smaller than 100 nm, the tumbling of the vesicles and the lateral diffusion of phospholipids at the vesicle surface, both contribute to the orientational averaging of the phosphate CSA.

As discussed already by Burnell *et al.* (*21*), the characteristic time τ for the reorientation of a phospholipid in a vesicle can be calculated by the formula

$$\frac{1}{\tau} = \frac{6}{r^2}\,(D_t + D_{diff}) = \frac{1}{\tau_t} + \frac{1}{\tau_{diff}},$$

where $D_t = kT/8\pi r\eta$ is the rotational diffusion coefficient of the vesicles, η is the medium viscosity, and D_{diff} is the rate of phospholipid lateral diffusion. Estimates can be made of the relative contributions of vesicle tumbling and of lipid surface diffusion. In the case of SUVs, the radius is approximately 20 nm; at 25°C in pure water, with $D = 1 \times 10^{-8}$ $cm^2\ s^{-1}$ (*31*) and $\eta = 0.89$ mPa s (''Handbook of Chemistry and Physics''), one finds that $\tau_t = 7 \times 10^{-6}$ and $\tau_{diff} = 6 \times 10^{-5}$ s, thus $\tau \approx 6 \times 10^{-6}$ s, with the main contribution to the averaging originating from vesicle tumbling. As the vesicles get progressively larger, τ increases. For LUVs, under the same conditions, $\tau_t \approx 1 \times 10^{-4}$ s, and $\tau_{diff} \approx 5 \times 10^{-4}$ s. In the latter case, τ is too long to narrow significantly the lines and even increasing the temperature to 40°C is insufficient (see Fig. 2b). Yet, the spontaneous tumbling is on a time scale comparable to that of the rotor's motion ($\approx 10^{-4}$ s), which efficiently averages the CSA in the case of MLVs. Thus, Brownian motion at the rate of the rotor's motion reduces the efficiency of the sample spinning.

By increasing the viscosity of the solution with glycerol, we decrease the spontaneous rotation rate of the LUVs until it no longer interferes with the averaging caused by the sample spinning. This spectacular result is to some extent surprising. Indeed if, following Burnell *et al.* (*21*), one assumes that glycerol has no effect on the lateral diffusion of lipids, then τ should be dominated by the lateral diffusion and remain in the range 10^{-4}–10^{-5} s. In fact, because the effect of vesicle tumbling on the rate of lipid rotational motion varies as r^{-3}, and of lateral diffusion as r^{-2}, diffusion eventually will become more important as vesicle size increases, even in pure water. In other words, the random motion caused by lateral diffusion should become predominant over tumbling when the viscosity is increased as well as the size of the vesicles. Therefore, in order to understand our data, one must assume that 50% glycerol does reduce to some extent the rate of diffusion of the lipids. Lateral diffusion may be a residual limitation in the efficient averaging of the CSA. This can be inferred from our finding that the addition of cholesterol, which can affect only lateral diffusion, has a measurable effect on the line narrowing (Fig. 1).

Increasing the concentration of glycerol might allow us to obtain narrower peaks. However, possible effects of glycerol on the shape of the LUVs are a concern. Glycerol can be responsible for partial dehydration of the lipid head groups. The perturbing effect of glycerol becomes severe at high concentrations. For example, Fenske and Cullis have shown that the order-parameter profile becomes reduced over the whole length of the chain (*22*). To verify sample integrity, electron cryomicroscopy was performed on 100 nm

LUVs composed of EPC/EPG (1:1 wt) in glycerol and it showed undistorted LUVs.

Note that the line broadening which appears with LUVs cannot be attributed to a vortex formed when spinning the liquid sample. A vortex would create a very inhomogeneous sample resulting in line broadening. However, SUVs and MLV suspensions are also liquid samples and their linewidth was not broadened by the spinning.

ACKNOWLEDGMENTS

The authors acknowledge the assistance of Drs. P. Fellmann and D. Warschawski for the NMR, Mrs. P. Hervé for the control of the lipid purity, Dr. Gulik for performing some freeze fracture electron microscopy on LUVs samples. This work was supported by grants from the Université Paris 7, the Centre National de la Recherche Scientifique (UPR 9052), the Institut National de la Santé et de la Recherche Médicale, the Association pour la recherche contre le Cancer, and the EEC (BIO2-CT93-0348).

REFERENCES

1. P. R. Cullis, L. D. Mayer, M. B. Bally, T. D. Madden, and M. J. Hope, *Adv. Drug Delivery Rev.* **3,** 267 (1989).
2. D. D. Lasic, *Biochem. J.* **256,** 1 (1988).
3. C. H. Huang, *Biochemistry* **8,** 344 (1969).
4. M. J. Hope, M. B. Bally, G. Webb, and P. R. Cullis, *Biochim. Biophys. Acta* **812,** 55 (1985).
5. L. D. Mayer, M. J. Hope, and P. R. Cullis, *Biochim. Biophys. Acta* **858,** 161 (1986).
6. J. Seelig and A. Seelig, *Q. Rev. Biophys.* **13,** 19 (1980).
7. J. H. Davis, *Biochim. Biophys. Acta* **737,** 117 (1983).
8. R. L. Smith and E. Oldfield, *Science* **225,** 280 (1984).
9. M. Bloom, E. Evans, and O. G. Mouritsen, *Q. Rev. Biophys.* **24,** 293 (1991).
10. D. A. Tyrrell, T. D. Heath, C. M. Coley, and B. E. Ryman, *Biochim. Biophys. Acta* **457,** 259 (1976).
11. P. R. Harrigan, K. F. Wong, T. E. Redelmeier, J. J. Wheelerand, and P. R. Cullis, *Biochim. Biophys. Acta* **1149,** 329 (1993).
12. S. J. Eastman, M. J. Hope, K. F. Wong, and P. R. Cullis, *Biochemistry* **31,** 4262 (1992).
13. D. Chapman, V. B. Kamat, J. De Gier, and S. A. Penkett, *J. Mol. Biol.* **31,** 101 (1968).
14. E. G. Finer, A. G. Flook, and H. Hauser, *Biochim. Biophys. Acta* **260,** 59 (1972).
15. M. P. Sheetz and S. I. Chan, *Biochemistry* **11,** 4573 (1972).
16. B. De Kruijff, P. R. Cullis, and G. K. Radda, *Biochim. Biophys. Acta* **406,** 6 (1975).
17. J. M. Neumann, A. Zachowski, S. Tran-Dinh, and P. F. Devaux, *Eur. Biophys. J.* **11,** 219 (1985).
18. V. V. Kumar, B. Malewicz, and W. J. Baumann, *Biophys. J.* **55,** 789 (1989).
19. M. A. Swairjo, B. A. Seaton, and M. F. Roberts, *Biochim. Biophys. Acta* **1191,** 354 (1994).
20. S. P. Bhamidipati and J. A. Hamilton, *Biochemistry* **34,** 5666 (1995).
21. E. E. Burnell, P. R. Cullis, and B. De Kruijff, *Biochim. Biophys. Acta* **603,** 63 (1980).
22. D. B. Fenske and P. R. Cullis, *Biophys. J.* **64,** 1482 (1993).
23. E. Oldfield, J. L. Bowers, and J. Forbes, *Biochemistry* **26,** 6919 (1987).
24. J. Forbes, C. Husted, and E. Oldfield, *J. Am. Chem. Soc.* **110,** 1059 (1988).
25. C. W. B. Lee and R. G. Griffin, *Biophys. J.* **55,** 355 (1989).
26. H. N. Halladay, R. E. Stark, S. Ali, and R. Bittman, *Biophys. J.* **58,** 1449 (1990).
27. M. M. Maricq and J. S. Waugh, *J. Chem. Phys.* **70,** 3300 (1979).
28. J. R. Long, B. Q. Sun, A. Bowen, and R. G. Griffin, *J. Am. Chem. Soc.* **116,** 11,950 (1994).
29. M. Roux, T. Huynh-Dinh, J. Igolen, and Y. Prigent, *Chem. Phys. Lipids* **33,** 41 (1983).
30. A. L. Van Geet, *Anal. Chem.* **42,** 679 (1970).
31. P. Devaux and H. M. McConnell, *J. Am. Chem. Soc.* **94,** 4475 (1972).